Acta Chemica Scandinavica, 1995: 49: 28–35
Printed in Belgium – all rights reserved

ACTA
CHEMICA SCANDINAVICA
ISSN 0904–213X

Kinetics and Equilibrium Constant of the Reversible Reaction $ClO + ClO + M \rightleftharpoons Cl_2O_2 + M$ at 295 K

Thomas Ellermann,[a,†] Klas Johnsson,[a] Anders Lund[b,*] and Palle Pagsberg[a]

[a]Chemical Reactivity Section, Environmental Science and Technology Department, Risø National Laboratory, DK-4000 Roskilde, Denmark and [b]Chemical Physics Laboratory, Department of Physics and Measurement Technology, University of Linköping, S-58183 Linköping, Sweden.

Ellermann, T., Johnsson, K., Lund, A. and Pagsberg, P., 1995. Kinetics and Equilibrium Constant of the Reversible Reaction $ClO + ClO + M \rightleftharpoons Cl_2O_2 + M$ at 295 K. – Acta Chem. Scand. 49: 28–35 © Acta Chemica Scandinavica 1995.

High yields of ClO radicals were obtained by pulse radiolysis of Cl_2O/Cl_2 mixed with Ar, SF_6, or CO_2 as bath gases. The kinetics of ClO was studied directly by monitoring the transient absorption signals at 277.2 nm. ClO was found to decay towards an equilibrium concentration in accordance with the reversible reaction $ClO + ClO + M \rightleftharpoons Cl_2O_2 + M$. The rate constants of the forward and reverse reactions were derived by computer modelling of the experimental curves. The rate constant of the forward reaction was found to be pressure-dependent, and the following values were obtained at a total pressure of 1 bar and with different third bodies at 295 K: $k_{2f} = (2.5 \pm 0.5) \times 10^{-13}$ (M = Ar), $(4.4 \pm 0.9) \times 10^{-13}$ (M = SF_6) and $(4.7 \pm 0.9) \times 10^{-13}$ (M = CO_2) in units of cm^3 $molecule^{-1}$ s^{-1}. Based on computer simulations of the observed relaxation kinetics a value of the equilibrium constant at 295 K, $K_{eq} = (6.4 \pm 1.6) \times 10^{-15}$ cm^3 $molecule^{-1}$, was obtained for the SF_6 and Ar systems.

Molina and Molina suggested in 1987[1] the existence of an unrecognized catalytic ozone destruction cycle which as crucial steps involved the formation and photolysis of the ClO dimer, reactions (2) and (3):

$$2 \times (Cl + O_3 \rightarrow ClO + O_2) \quad (1)$$

$$ClO + ClO + M \rightarrow Cl_2O_2 + M \quad (2)$$

$$Cl_2O_2 + h\nu \rightarrow ClOO + Cl \quad (3)$$

$$\frac{ClOO + M \rightarrow Cl + O_2 + M}{\text{net: } 2\,O_3 \rightarrow 3\,O_2} \quad (4)$$

This catalytic cycle has been shown to be very important for the development of the Antarctic springtime ozone depletion[2] first reported by Farman *et al.*[3] The ClO dimer mechanism is particularly effective at Antarctica owing to the very low temperatures. Formation of polar stratospheric clouds gives rise to very high ClO concentrations,[4] thereby enhancing the rate of formation of the ClO dimer. The stability of the dimer at low temperatures favors the photolysis of the dimer at the expense of the thermal dissociation of the ClO dimer back to two ClO radicals.[5] Model calculations have shown that the ClO dimer mechanism may account for as much as 70% of the observed stratospheric ozone degradation during the Antarctic spring.[6] Therefore a thorough understanding of the chemistry of the ClO dimer is important.

Since Molina and Molina suggested the ClO dimer mechanism, many aspects of the chemistry of the ClO dimer have been investigated both experimentally and theoretically.[1,7–20] A detailed study of the bimolecular and termolecular channels of the ClO + ClO reaction has appeared very recently.[21] *Ab initio* calculations by McGrath *et al.*[10] have shown that several isomers of the ClO dimer might exist, with $ClClO_2$ being slightly less energetically favorable than the most stable isomer, the symmetrical peroxide form ClOOCl. Birk *et al.*[14] studied experimentally the products of the ClO dimerisation reaction employing submillimetre microwave spectroscopy and found ClOOCl to be a major product and the only detectable isomer of the ClO dimer. This is supported by the results of DeMore and Tschuikow-Roux[16] who, from the absence of OClO and Cl_2O_3 as products of the dimerisation reaction, concluded that ClOClO and probably $ClClO_2$ cannot be stabilized at temperatures of 195 K or above. The UV absorption spectrum of the ClOOCl dimer has been shown by several studies to consist of a broad band in the range 190–390 nm with a local minimum at 220 nm and a maximum at 245 nm, with the absorption cross-

† Present address: Department of Emissions and Air Pollution, National Environmental Research Institute, DK 4000 Roskilde, Denmark.
* To whom correspondence should be addressed.

section determined by four studies to fall in the range $(6.4–6.8) \times 10^{-18}$ cm^2 molecule^{-1}.[8,13,16,20] The kinetics of the dimerisation reaction has also been studied by several groups,[9,11,15,21] with a factor of 3 in discrepancy between the results for the low-pressure rate constant with $M = N_2/O_2$. However, better agreement has been obtained between recent results reported by Trolier *et al.*[15] and Sander *et al.*[11]

To our knowledge only three determinations of the equilibrium constant for the equilibrium between the ClO monomer and dimer have been reported. Basco and Hunt[7] employed a flash-photolysis apparatus combined with UV spectroscopy to determine the UV spectrum of the dimer, the rate of dimerisation and the equilibrium constant; $K_{eq}(295\ K) = (5.2 \pm 0.2) \times 10^{-15}$ cm^3 molecule^{-1}. However, this value has to be questioned because the determination of K_{eq} relies on the absorption cross-section for Cl_2O_2, and the UV spectrum did not agree with recent observations.[8,13,16,20] The same technique was employed by Sanders *et al.* to measure K_{eq} over the temperature interval 260–310 K.[21] Cox and Hayman[8] used a static photolytic system coupled with UV spectroscopy to record absorbance changes on a timescale of minutes. From their interpretation of the complex system involving slow secondary chemistry and wall reactions they derived the equilibrium constant as function of temperature; $K_{eq}(295\ K) = (6.7 \pm 0.7) \times 10^{-15}$ cm^3 molecule^{-1}. Again the determination was based on determination of $\sigma_{Cl_2O_2}$. The spectrum measured by Cox and Hayman is in agreement with the recently reported UV spectrum for Cl_2O_2.[13,16,20]

The aim of the present investigation has been a redetermination of the equilibrium constant for the reversible reaction between the ClO monomer and dimer employing a different and more direct technique, i.e. pulse radiolysis combined with time-resolved ultraviolet spectroscopy. With this method a ClO concentration up to 3.6×10^{15} molecule cm^{-3} could be obtained, i.e. an order of magnitude higher than with flash photolysis.[15] In addition we have determined the pressure-dependent rate constant for the dimerisation reaction at 295 K and 1 bar with three different bath gases, M = Ar, SF_6 or CO_2. The pressure dependence of the rate constant with M = Ar was studied in the range of $p(Ar) = 0.25–1.0$ bar.

Experimental

The ClO radicals were produced by pulse radiolysis of gas mixtures of Cl_2O/Cl_2 diluted in CO_2, SF_6, or Ar. The formation and decay of the radicals were followed by transient UV absorption spectroscopy. The experimental set-up has previously been described in detail,[22–24] and only a brief summary will be given here.

Gas mixtures were prepared by admitting one component at a time and reading the corresponding partial pressure with a MKS Baratron absolute electronic membrane manometer with a resolution of 10^{-5} bar. The gas mixtures were irradiated by a 30 ns pulse of 2 MeV electrons from a Febetron 705B electron accelerator. Variation in the radiation dose was achieved by the use of stainless-steel electron-beam attenuators. Calibration of attenuation factors in terms of fractions of the maximum dose was determined by ozone dosimetry, i.e. by monitoring the yield of O_3 produced by pulse radiolysis of O_2 using the well known value of $\sigma(O_3) = 1.15 \times 10^{-17}$ cm^2 molecule^{-1} at 254 nm. A pulsed 150 W xenon lamp stabilized by optical feedback provided a high intensity of ultraviolet light which was needed in order to obtain a good signal-to-noise ratio of transient species absorbing in the range 200–300 nm. Using lamp pulses with a duration of about 10 ms a 50-fold increase was obtained in the light intensity, which remained constant within 5% controlled by the optical feedback from a beam splitter. Via an optical system composed of Suprasil lenses the analyzing light beam entered the sample cell, where a set of internal spherical mirrors provided optical path lengths of 40, 80 or 120 cm through the reaction zone. The spectral features were analyzed by a 1 m grating monochromator applying a 1200 line mm^{-1} grating, which gives a reciprocal dispersion of 8 Å mm^{-1}. Accurate wavelength calibrations were carried out using reference emission lines from a PEN-RAY mercury lamp.

The light intensity was monitored with a fast photomultiplier, and the output signals were digitized with a Biomation 8100 transient recorder collecting 2000 equidistant data points with a minimum of 10 ns between samples. Conversion of raw data into transient absorption versus time and display of kinetically relevant functions were accomplished with an on-line computer. The experimental kinetic curves were analyzed by detailed computer modelling of the reaction mechanism using the chemical kinetics program CHEMSIMUL.[25]

Ultra-high-purity argon (99.998%) was obtained from L'air Liquide. CO_2 (99.5%) was obtained from AGA and SF_6 (99.9%) from Hede Nielsen. The gases were used as received. Cl_2O was synthesised[26] by O. Jørgensen at Risø Chemistry Department. The purity of the synthesised gas was analyzed by UV spectroscopy. The composition of fresh gas samples was found to be approximately 60% Cl_2O and 40% Cl_2, based on values of $\sigma_{Cl_2O}(277.2\ nm) = (1.31 \pm 0.07) \times 10^{-18}$ cm^2 molecule^{-1} derived as an average of three determinations by Lin,[27] Knauth *et al.*[28] and Molina and Molina,[29] and the value of $\sigma_{Cl_2}(330\ nm) = 25.6 \times 10^{-20}$ cm^2 molecule^{-1} recommended by the most recent NASA data evaluation.[30] The Cl_2O/Cl_2 sample was stored overnight in liquid nitrogen, and during the experiments the sample was cooled in dry ice. Before the experiments the Cl_2O/Cl_2 sample was frozen in liquid nitrogen on the vacuum line, and the more volatile impurities were pumped off.

Results

Formation of ClO. ClO radicals were produced by pulse radiolysis of gas mixtures containing a small mole fraction of Cl_2O/Cl_2 mixed with Ar, SF_6 or CO_2 as bath gas

at a total pressure of 1 atm. The reactions leading to the formation of ClO in the three different systems are summarized below.

SF_6 system:

$$SF_6 \xrightarrow{e^-} F + \text{products} \quad (5)$$

$$F + Cl_2O \rightarrow FCl + ClO \quad (6)$$

$$F + Cl_2 \rightarrow FCl + Cl \quad (7)$$

$$Cl + Cl_2O \rightarrow Cl_2 + ClO \quad (8)$$

Ar system:

$$Ar \xrightarrow{e^-} Ar^* \quad (9)$$

$$Ar^* + Cl_2O \rightarrow Ar + Cl + ClO \quad (10)$$

$$Ar^* + Cl_2 \rightarrow Ar + Cl + Cl \quad (11)$$

$$Cl + Cl_2O \rightarrow Cl_2 + ClO \quad (8)$$

CO_2 system:

$$CO_2 \xrightarrow{e^-} CO + O \quad (12)$$

$$O + Cl_2O \rightarrow ClO + ClO \quad (13)$$

$$O + Cl_2 \rightarrow Cl + ClO \quad (14)$$

$$O + ClO \rightarrow Cl + O_2 \quad (15)$$

$$Cl + Cl_2O \rightarrow Cl_2 + ClO \quad (8)$$

SF_6 and Ar systems. Figure 1 shows an example of the ClO absorption signals at 277.2 nm observed by pulse radiolysis of a gas mixture containing a small mole fraction of Cl_2O/Cl_2 in Ar. The transient absorption signal is composed of three components because of overlap between the ultraviolet absorption spectra of ClO, Cl_2O and Cl_2O_2 in the range 200–300 nm. The insert in Fig. 1 shows the shape of the (11,0) band of ClO at 277.2 nm recorded with a spectral bandpass of 0.2 nm and an optical path length of 120 cm. With this spectral resolution the apparent bandwidth is approximately 1 nm. ClO has the largest absorption cross-section at 277.2 nm, where values of $\sigma_{ClO} = 6.79$ at 0.3 nm and $\sigma_{ClO} = 7.27$ at 0.013 nm resolution[31] in units of 10^{-18} cm^2 molecule^{-1} have been reported. In this study the value $\sigma_{ClO} = 7.2 \times 10^{-18}$ cm^2 molecule^{-1} was adopted,[32] in agreement with our experimental estimate, see below. At this wavelength $\sigma_{Cl_2O_2} = 1.92$,[30] and $\sigma_{Cl_2O} = (1.31 \pm 0.07)$[27–29] in units of 10^{-18} cm^2 molecule^{-1}.

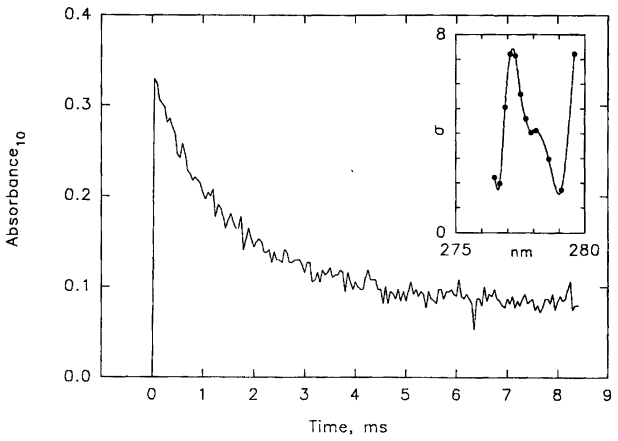

Fig. 1. Absorption transients recorded at 277.2 nm by irradiation, at relative dose=0.53, (see text) of gas mixtures of 0.3 mbar Cl_2O, 0.2 mbar Cl_2 and 1000 mbar Ar. The insert shows part of the ClO fine structure around the (11,0) band at 277.2 nm. The units of σ are 10^{18} cm^2 molecule^{-1}.

The maximum of the absorption signal at 277.2 nm shown in Fig. 1 can therefore be assigned to the formation of ClO taking into account the consumption of Cl_2O in the reactions (8) and (10). As shown in Fig. 2A the yields of ClO obtained in the SF_6 system are almost a factor of two higher than the yields observed with the same irradiation doses in the Ar system, i.e. $(1.90 \pm 0.07) \times 10^{15}$ cm^{-3} at a relative dose of 0.53. The subsequent decay (Fig. 1) corresponds to relaxation towards an equilibrium mixture of ClO and $(ClO)_2$ in accordance with the reversible association reaction (2).

The measurement of the absolute initial ClO concentration, which is a key parameter in the determination of K_{eq}, is not straightforward owing to the absorbance from both ClO and Cl_2O. The structure of the ClO spectrum (see insert in Fig. 1) makes the observed ClO absorption cross-sections highly dependent on instrumental resolution. The assumed stoichiometry for the conversion of Cl_2O into ClO also affects the results. Therefore a determination of the maximum absorbance as function of irradiation dose was carried out. The linearity between maximum absorbance and irradiation dose for relative dose ≤ 0.53 in the SF_6 and Ar system (Fig. 2A) indicates that all the fluorine atoms react either with Cl_2O or Cl_2, suggesting a one-to-one stoichiometry between Cl_2O and ClO. Under these conditions the yield of ClO equals the initial yield of F atoms produced by pulse radiolysis of SF_6. The rate constants for the F atom reactions (6) and (7) and reaction (8) are such that ClO is instaneously formed on the timescale of Fig. 1. For the purpose of modelling, equal rates for reactions (6) and (7) were assumed. At the highest doses a fraction of the fluorine atoms and excited argon atoms is lost in secondary reactions.

The yield of F atoms was determined by the titration reaction $F + CH_4 \rightarrow HF + CH_3$, which was initiated by pulse radiolysis of CH_4/SF_6 mixtures. From the maximum of the transient CH_3 absorption signal monitored at 216.4 nm combined with the reported value of the absorption cross-section,[36] the primary yield of F atoms was determined as $[F]_0 = [CH_3]_{max} = A(216.4)/\sigma(CH_3) \times L$. L is the optical path length in cm. The yield of F atoms was found to be a linear function of the

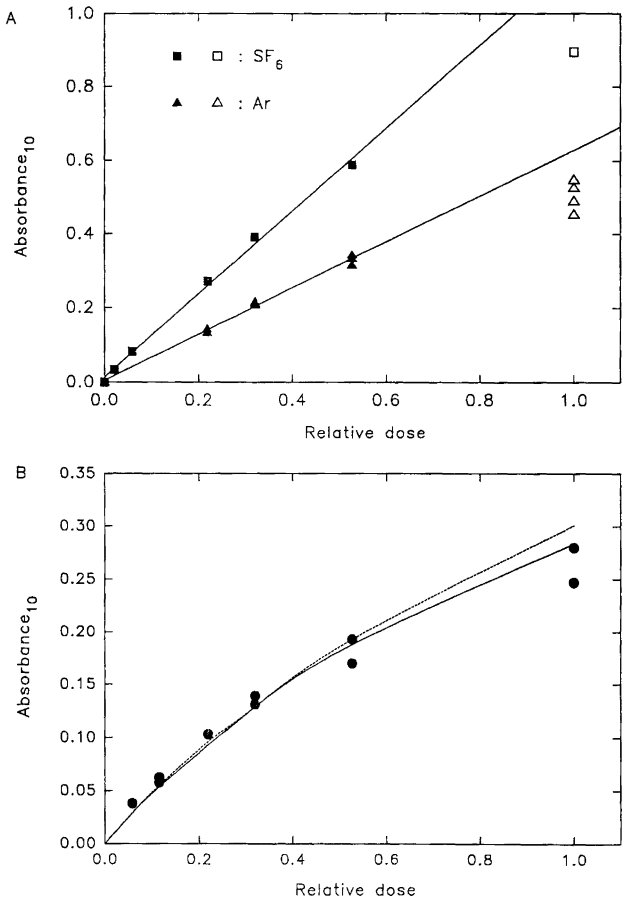

Fig. 2. Maximum absorbance at 277.2 nm plotted as function of irradiation dose for the Ar and SF_6 systems (A) and for the CO_2 system (B). All data were obtained by irradiation of gas mixtures of 0.3 mbar Cl_2O, 0.2 mbar Cl_2 and 1000 mbar of the third body. The solid lines in (A) are determined by least-squares analysis of the data at relative dose 0.53 and below. The lines in (B) have been determined by simulation of the CO_2 reaction mechanism (Table 1). Dashed line: without ClO decay; solid line: ClO decay included.

irradiation dose. From the relative magnitude of the absorption signals of ClO and CH_3 produced in the titration reaction at a relative irradiation dose of 0.53 a value of $\sigma(ClO)_{277.2\ nm} = (7.25 \pm 0.40) \times 10^{-18}$ cm^2 molecule^{-1} at a bandpass of 0.2 nm was derived. The overall uncertainty of about 6% was estimated taking into account uncertainties in the observed transient absorption signals combined with uncertainties in the reported values of $\sigma(CH_3)$[36] and $\sigma(Cl_2O)$.[27-29] Similar results were obtained by comparison of $\sigma(ClO)$ and $\sigma(CH_3O_2)$,[37] where the methylperoxy radical was produced by pulse radiolysis of $SF_6/CH_4/O_2$ mixtures. The yields of F atoms determined by the two different titration reactions based on CH_3 and CH_3O_2 absorption signals were found to be identical within a standard deviation of 5% in series of repetitive experiments. The scatter in the transient absorption measurements is mainly due to variations in the irradiation doses. Based on this determination the value of $(ClO)_{277.2\ nm} = 7.2 \times 10^{-18}$ cm^2 molecule^{-1} has been obtained, in agreement with results which have been reviewed by Watson.[32] However, in order to carry out a quantitative analysis of the observed kinetic features one must also take into account the absorption of the dimer using the recommended value of $\sigma(Cl_2O_2)$.[30]

CO_2 system For the CO_2 system a clear deviation from linearity between maximum absorbance and relative dose is observed (Fig. 2B). This is due to the very fast reaction (15) between the oxygen atoms and ClO, which was verified by computer simulations of the relevant reactions shown in Table 1. The chlorine atom regenerates ClO in reaction (8). The overall result will therefore be a reduction of the number of ClO radicals for each oxygen atom below two which would be obtained if all O atoms were consumed in reaction (13). The initial yield of O atoms produced by pulse radiolysis of CO_2 was determined by monitoring the yield of ozone produced in the titration reaction $O + O_2 \rightarrow O_3$ observed by radiolysis of CO_2/O_2 mixtures. From the absorption signal of O_3 monitored at 254 nm combined with a consensus value of $\sigma_{O_3} = 1.15 \times 10^{-17}$ cm^2 molecule^{-1},[30] an initial yield of $[O]_0 = [O_3]_{max} = (7.8 \pm 0.5) \times 10^{14}$ cm^{-3} was derived corresponding to the maximum irradiation dose. Using this value in the model calculations we have been able to reproduce the experimental yields of ClO shown in Fig. 2B. The dashed line represents the simulated maximum absorbances when only the reactions (8) and (12)–(15) were taken into account. Employing the complete set of ClO

Table 1. Rate constants used in the simulations.

Reaction		$k_{295\,K}$ /cm^3 molecule^{-1} s^{-1}	Ref.
CO_2 system:			
(8) $Cl + Cl_2O$	$\rightarrow ClO + Cl_2$	$(9.8 \pm 2.0) \times 10^{-11}$	30
(13) $O + Cl_2O$	$\rightarrow 2\ ClO$	$(3.5 \pm 1.4) \times 10^{-12}$	30
(14) $O + Cl_2$	$\rightarrow ClO + Cl$	4.2×10^{-13}	35
(15) $O + ClO$	$\rightarrow Cl + O_2$	$(3.8 \pm 0.8) \times 10^{-11}$	30
SF_6 system:			
(6) $F + Cl_2O$	$\rightarrow FCO + ClO$	$(1.4 \pm 0.4) \times 10^{-10}$	33
(7) $F + Cl_2$	$\rightarrow FCl + Cl$	$1.4 \pm \times 10^{-10}$	[a]
(8) $Cl + Cl_2$	$\rightarrow Cl_2 + ClO$	$(9.8 \pm 2.0) \times 10^{-11}$	30
ClO decay:			
(2f) $ClO + ClO + M$	$\rightarrow Cl_2 + M$	see Table 3	
(2r) $Cl_2 + M$	$\rightarrow ClO + ClO + M$	see Table 3	
(4) $ClOO + M$	$\rightarrow Cl + O_2 + M$	2×10^7	[b]
(16) $ClO + ClO$	$\rightarrow ClOO + Cl$	$(7.2 \pm 1.6) \times 10^{-15}$	31
(17) $ClO + ClO$	$\rightarrow OClO + Cl$	$(7.3 \pm 2.6) \times 10^{-15}$	31
(18) $ClO + ClO$	$\rightarrow Cl_2 + O_2$	$(7.3 \pm 1.8) \times 10^{-15}$	31
(19) $Cl + Cl_2O_2$	$\rightarrow ClOO + Cl_2$	1.6×10^{-10}	8
(20) $Cl + OClO$	$\rightarrow ClO + ClO$	$(5.8 \pm 1.5) \times 10^{-11}$	30

[a] Assumed to be equal to k_6. [b] In units of s^{-1}. The rate constant at 1 bar total pressure is calculated from K_{eq} of $Cl + O_2 \leftrightarrow ClOO$ and k_{-4}.[30]

decay channels including reactions (2) and (16)–(18) listed in Table 1 the yield curve represented by the solid line was obtained, in good agreement with the experimental results.

Determination of K_{eq}. The initial decay of ClO is governed by the reversible dimerisation reaction (2)

$$ClO + ClO + M \rightarrow Cl_2O_2 + M \quad (2f)$$

$$Cl_2O + M \rightarrow ClO + ClO + M \quad (2r)$$

Subsequently the equilibrium mixture of ClO and Cl_2O_2 is consumed in slower irreversible reactions, i.e. (16)–(18), which have been taken into account in our detailed computer simulations. A first estimate of the equilibrium constant was carried out by a simple analysis based on measurements of the initial concentration of ClO and the concentration of ClO when the equilibrium has been established.

Using the following shorthand symbols for the concentrations of the monomer and the dimer, $M_0 = [ClO]_0$, $M = [ClO]_{eq}$ and $D = [Cl_2O_2]_{eq}$, we combine the equilibrium equation (I) and the material balance for ClO, eqn. (II), to obtain eqn. (III), which was used for the evaluation of the equilibrium constant.

$$K_{eq} = D/M^2 \quad (I)$$

$$M_0 = M + 2D \quad (II)$$

$$K_{eq} = (M_0 - M)/2M^2 \quad (III)$$

The initial concentration of ClO was derived from the maximum of the transient absorption signal at 277.2 nm, taking into account the consumption of Cl_2O, i.e. $M_0 = A_{max}/(\sigma_{ClO} - \sigma_{Cl_2O})L$, where L is the optical path length. Likewise at equilibrium we include the contribution from the dimer, which also contributes to the absorption.

At 277.2 nm the ClO absorption cross-section is four times higher than the Cl_2O_2 absorption cross-section. Thus, in the limiting irreversible case of 100% conversion of ClO into Cl_2O_2 the transient absorption should decrease to about 13% of the initial value.

Figure 3 shows three examples of the transient absorption signals at 277.2 nm observed by pulse radiolysis of $SF_6/Cl_2O/Cl_2$ mixtures. The upper curve was obtained with a relative dose of 0.53. The decay of ClO towards equilibrium takes place on a timescale of a few milliseconds, during which the absorption signal is reduced to about 30% of the maximum value. For the two lower curves, obtained with relative doses of 0.32 and 0.22, the signals are reduced to 37% and 32% of the maximum values. This trend is in qualitative agreement with eqn. (III), predicting a lower relative equilibrium concentration, M/M_0 with increasing total concentration, $M_0 = M + 2D$. Using this simple analysis with SF_6 as bath gas, and the initial $[ClO]_0$ and equilibrium $[ClO]_{eq}$ concentrations obtained from the experimental decay curve at a relative dose of 0.53 (Fig. 3) an equilibrium constant of $K_{eq} = k_{2f}/k_{2r} = 6.0 \times 10^{-15}$ cm^3 molecule^{-1} was estimated.

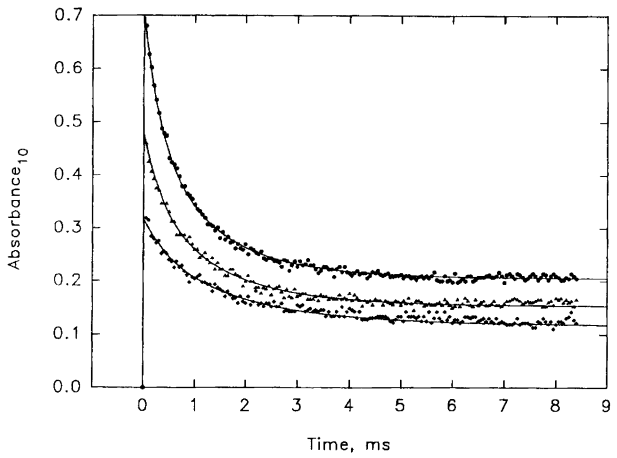

Fig. 3. Comparison of simulated and experimental absorption transients at 277.2 nm. The experimental data were obtained by radiolysis of 0.3 mbar Cl_2O, 0.2 mbar Cl_2, and 1000 mbar SF_6 at irradiation dose 0.53 (●), 0.32 (▲), and 0.22 (◆). The data were corrected for decrease in absorbance due to consumption of Cl_2O.

A similar analysis was attempted with Ar and CO_2 as bath gases. However, owing to the lower radical yields obtained in these systems the relaxation toward equilibrium for the ClO dimer formation took place on a longer timescale. Thus, in a time of 10 ms, which is the limit of the pulsing device for the Xe lamp, the equilibrium was not established, and the simple method for the determination of K_{eq} could not be used. Instead detailed computer simulations of the complete reaction mechanism had to be employed to determine the values of K_{eq} as well as the forward and reverse rate constants.

Simulations. A quantitative evaluation of the equilibrium constant and the rates of the forward and reverse reactions was achieved by detailed computer simulations of the chemical reaction mechanism. Model traces of transient absorption versus time curves were obtained by plotting a weighted sum of Cl_2O, ClO and Cl_2O_2 time profiles generated by the CHEMSIMUL program using values of the absorption cross-sections for these species mentioned above. The reaction mechanisms are shown in Table 1. The calculated absorption transients were compared directly with the experimentally observed absorption transients, and the rate constants k_{2f} and k_{2r} were adjusted for the best visual fit. This method has the advantage that it makes use of all the information in the ClO decay towards equilibrium, while the simple method described above only employs the absorbance at maximum ClO concentration and at equilibrium. As shown in Fig. 3 the model traces could be fitted to the experimental curves within the signal-to-noise ratio using the same set

of rate constants for the three different irradiation doses.

k_{2f} and k_{2r} are the only important unknown parameters in the simulations of the three reaction mechanisms. For the CO_2 system all rate constants except k_{2f} and k_{2r} were obtained from the literature. For both the Ar and SF_6 systems there are unknown rate constants among some of the reactions producing ClO. However, the observed formation of ClO in both systems is much faster than the ClO decay. For the Ar system only the ClO decay was taken into account, omitting the reactions (8)–(11), which describe the very fast energy transfer from metastable Ar to Cl_2O and Cl_2, cleavage of excited Cl_2O and Cl_2, and reaction of the Cl atoms with Cl_2O. The production of fluorine atoms in the SF_6 system occurs on a timescale comparable to the timescale of the irradiation pulse. Reaction (6) between fluorine atoms and Cl_2O has recently been investigated by Stevens and Anderson,[33] who reported a rate coefficient of $k_{295\ K} = (1.4 \pm 0.4) \times 10^{-10}$ cm^3 molecule^{-1} s^{-1}.

The equilibrium constants $K_{eq} = k_{2f}/k_{2r}$, determined by computer modelling, are listed in Table 2. The results obtained with SF_6 and Ar as bath gases and at varying irradiation doses are in agreement within 10% of the average value. The values obtained with CO_2 as bath gas are significantly lower, in particular at the lower irradiation doses. The reason for this discrepancy is not yet clear, but one cannot rule out additional reactions which have not been taken into account in the computer simulations. With this in mind the average value of $K_{eq} = 6.4 \times 10^{-15}$ cm^3 molecule^{-1} obtained from the somewhat simpler SF_6 and Ar-systems should be considered more reliable. This value is also in fair agreement with previous experimental results reported by Basco and Hunt,[7] Cox and Hayman[8] and Nicholaisen *et al.*[21]

Rate constants for the dimerisation reaction. Mean values of k_{2f} and k_{2r} for 295 K and 1 bar total pressure determined by the computer simulations are listed in Table 3. The differences in the rate coefficients for the ClO combination reaction observed with CO_2, SF_6 and Ar as bath gases are thought to reflect differences in the third body efficiencies of these bath gases.

Table 2. Equilibrium constant determined by simulation of the three different chemical system at 295 K. The literature data refer to the same temperature.

	$K_{eq}/10^{-15}$ cm^3 molecule^{-1}		
Relative dose	CO_2	SF_6	Ar
1.0	5.05	–	–
0.53	4.75	6.8	6.2
0.32	4.75	6.8	6.2
0.32	4.75	6.8	6.2
0.22	–	5.9	–
Basco and Hunt:[7]	$(5.2 \pm 0.2) \times 10^{-15}$		
Cox and Hayman:[8]	$(6.7 \pm 0.7) \times 10^{-15}$		
Nickolaison *et al.*[21]	$10.4 \pm 1.0) \times 10^{-15}$		

Table 3. Rate constants k_{2f} and k_{2r} for M=CO_2, SF_6 and Ar.

	$k_{2f}/10^{-13}$ cm^3 molecule^{-1} s^{-1}			k_{2r}[a]/s^{-1}		
Relative dose	CO_2	SF_6	Ar	CO_2	SF_6	Ar
1.0	4.63	–	–	92	–	–
0.53	4.75	4.25	2.50	100	63	42
0.32	4.75	4.75	2.50	100	70	42
0.22	–	4.25	–	–	72	–
Mean	4.72	4.42	2.50	97	68	42

[a] Given as apparent second- and first-order rate constants at 1 bar total pressure.

The pressure dependence of the dimerisation reaction (2) was studied with Ar as the bath gas as shown in Fig. 4. The solid line represents a least-squares fit of the Troe parametrization of the fall-off curve of a termolecular reaction.[34] Using a limiting high-pressure rate constant of $k = (6 \pm 2) \times 10^{-12}$ cm^3 molecule^{-1} s^{-1} reported by Sander *et al.*[11] and a standard value[30] of the broadening factor, $F_c = 0.6$, a limiting low-pressure rate constant, $k_0 = 1.3 \times 10^{-32}$ cm^6 molecule^{-2} s^{-1}, was derived.

The experimental results obtained in CO_2 and SF_6 at a total pressure of 1 bar are also shown in Fig. 4, and third body efficiencies of 2.2 for M = (CO_2) and 2.1 for M = SF_6 have been estimated relative to 1.0 with M = Ar as reference bath gas.

In addition to the pressure-dependent dimerisation channel (2) we have considered the contribution from the irreversible bimolecular reactions (16)–(18) to the overall decay rate of ClO.

$$ClO + ClO \rightarrow Cl + ClOO \quad (16)$$

$$\rightarrow Cl + OClO \quad (17)$$

$$\rightarrow Cl_2 + O_2 \quad (18)$$

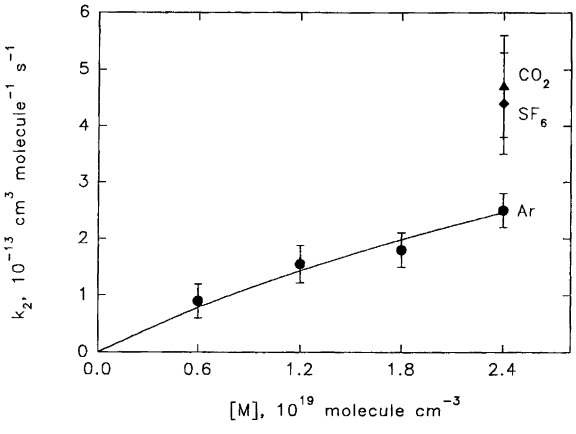

Fig. 4. Pressure dependence of k_{2f} with Ar as third body. The solid line represents a fit of the Troe parametrization to the data. The rate constants obtained with 1 bar CO_2 and 1 bar SF_6, respectively, are also shown.

The temperature dependence of these reactions has recently been determined.[21] From these data the dimerisation reaction (2) at 295 K is 10 times faster than the sum of the bimolecular channels. The bimolecular channels become important on longer timescales. On a timescale of seconds the majority of the excess Cl_2O is degraded via a slow chain initiated by chlorine atom formation in reactions (16) and (17). The chain is propagated by the following steps:

$$ClOO + M \rightarrow Cl + O_2 + M \quad (4)$$

$$Cl + Cl_2O \rightarrow Cl_2 + ClO \quad (8)$$

$$Cl + Cl_2O_2 \rightarrow Cl + ClOO \quad (19)$$

$$Cl + OClO \rightarrow ClO + ClO \quad (20)$$

Both reactions (19) and (20) are known to be fast at 295 K: $k_{19} = 1.06 \times 10^{-10}$ cm^3 molecule^{-1} s^{-1} [8] and $k_{20} = 5.8 \times 10^{-11}$ cm^3 molecule^{-1} s^{-1}.[30] A similar degradation of Cl_2O by a short-chain mechanism was observed by Basco and Hunt.[7] Detailed computer modelling was carried out using an extended reaction mechanism including reactions (16)–(20). The results confirmed that these reactions did not have any significant effect on the ClO and Cl_2O_2 concentrations during a timescale of 10 ms which was employed in our studies of the relaxation kinetics.

Discussion

Our results on the equilibrium constant for the ClO dimerisation reaction at 295 K are listed in Table 2 in comparison with previous experimental studies. The equilibrium constant reported by Basco and Hunt[7] may be uncertain within a factor of two because the value of K_{eq} was derived using a value of $\sigma_{Cl_2O_2}$ which differs by a factor of two in comparison with recent literature data.[8,13,16,20]

In order to estimate the uncertainties involved in the determination a simple analysis based on the analytical expression for K_{eq} [eqn. (III)] and computer simulations of the reaction mechanism, combined with sensitivity analysis based on curve fitting, have been employed. In the first case an uncertainty of the initial ClO concentration of $\pm 15\%$ in the determination of the fluorine atom yield, based on the titration reaction with CH_4, gives rise to a 20% uncertainty of K_{eq}. The absorption cross-sections of Cl_2O_2 from Cox and Hayman,[8] DeMore and Tschuikow-Roux[16] and Permien *et al.*[20] agree to within $\pm 5\%$. A change in $\sigma_{Cl_2O_2}$ of this magnitude gives an 8% change in K_{eq} when using the simple method. In the sensitivity analysis model traces were generated as a weighted sum of ClO, Cl_2O and Cl_2O_2 time profiles using the absorption cross-sections for these species and compared with the experimental curves shown in Fig. 3 taking into account uncertainties in the absorption cross-sections of ClO, Cl_2O_2 and Cl_2O. Based on this analysis the uncertainty of the equilibrium constant was estimated to be $\pm 28\%$. The uncertainty in the yield of ClO and the assumption of complete conversion of F atoms into ClO radicals via reactions (6)–(8) as suggested by the experimental results shown in Fig. 2, i.e. $[ClO]_{max} = [F]_0$ at relative irradiation doses ≤ 0.53 of the maximum, have also been considered.

We believe that an estimated uncertainty of $\pm 30\%$ is realistic in view of the good signal-to-noise ratio of the experimental decay curves combined with a reliable determination of the absolute radical yields.

The rate constants obtained in this work are listed in Table 4, together with literature data. The overall uncertainty of the rate constant of the forward reaction is estimated to be $\pm 20\%$ in this work. The simplest way to compare our values with the literature data would be at 295 K and 1 bar for different M. However, in several cases the parametrizations of the fall-off curves had to be used to extrapolate to room temperature and 1 bar. In view of this and of the differences in methods, the agree-

Table 4. Pressure dependence of k_2 at 295 K[a]

Ref.	M	$k_0/10^{-32}$ cm^6 molecule^{-2} s^{-1}	$k/10^{-12}$ cm^3 molecule^{-1} s^{-1}	$k_{1\,bar}$[b]$/10^{-13}$ cm^3 molecule^{1} s^{-1}
This work	Ar	1.3	6	(2.5±0.5)
	SF_6			(4.4±0.9)
	CO_2			(4.7±0.9)
Hayman[9]	N_2, O_2	(6.0±0.3)	–	3.0[c]
Sander[11]	Ar	0.9[d]	(6±2)	1.77
	O_2	1.71[d]	(6±2)	3.09
	N_2	(1.8±0.5)	(6±2)	3.23
Trolier[15]	He	(0.46±0.04)[e]	(8±1.3)	1.24
	O_2	(1.09±0.08)[e]	(8±1.3)	2.43
	N_2	(1.30±0.09[e]	(8±1.3)	2.80
	SF_6	(2.20±0.14)[e]	(8±1.3)	4.27

[a] $F_c = 0.6$ has been used in all the parametrizations. [b] The rate constants at 1 bar total pressure have been calculated from k_0 and k except from data of this work, where the direct measurements are given. [c] Taken from Fig. 1 in Ref. 9. [d] Assuming that the ratio 1.0 : 1.9 : 2.0 for Ar : O_2 : N_2 at 207 K[11] is valid at 295 K. [e] Included an intercept owning to departure from the standard Troe formalism.[15]

ment is considered satisfactory. The values obtained by Nicholaisen *et al.*[21] at 300 K and 1 bar of 3.10 and 5.59×10^{-13} cm^3 molecule with M = Ar and SF_6 are also in fair agreement with ours.

Conclusion

Pulse radiolysis of gas mixtures containing Cl_2O/Cl_2 in different bath gases, M = Ar, SF_6 and CO_2, was used to initiate three different ClO source reactions by which we obtained radical yields in the range of $[ClO]_0 = (0.1–3.6) \times 10^{15}$ molecule cm^{-3}.

Thanks to the high radical yields we have been able to study the transient absorption signals of ClO with good signal-to-noise ratios during the relaxation towards equilibrium on a timescale of 10 ms. The decay of ClO was monitored at 277.2 nm employing a spectral bandpass of 0.2 nm, which was selected to obtain a maximum absorption signal in agreement with the recommended value of $\sigma(ClO)$.[32] The experimental kinetic features could be quantitatively accounted for by detailed computer modelling of the relaxation towards the thermal equilibrium via the reaction $ClO + ClO + M = Cl_2O_2 + M$, taking into account also the overlap between the ultraviolet spectra of ClO, Cl_2O_2 and Cl_2O. Absolute values of the rate constants for the forward and reverse reactions as well as the equilibrium constant were derived on the basis of literature values of the absorption cross-sections of ClO, ClO_2 and Cl_2O_2. Good agreement with other measurements using different techniques have been obtained, indicating that the obtained equilibrium constant and the rate constants can be treated with confidence. The agreement between the results obtained with different experimental techniques is of importance for the modelling of stratospheric ozone chemistry.

Acknowledgement. We thank O. Jørgensen and S. Pedersen for their great help with the synthesis of the Cl_2O samples used in this work, and O. J. Nielsen for stimulating discussions of our experimental results. We gratefully acknowledge the financial support obtained from Stiftelsen Futura and from NFR during our participation in the EC Environmental Programme, contract no. EV5V-CT91-0016.

References

1. Molina, L. T. and Molina, M. J. *J. Phys. Chem. 91* (1987) 433.
2. Solomon, S. *Nature (London) 347* (1990) 347.
3. Farman, J. C., Gardiner, B. G. and Shanklin, J. D. *Nature (London) 315* (1985) 207.
4. Solomon, S., Garcia, R. R., Rowland, F. S. and Wuebbles, D. J. *Nature (London) 321* (1986) 755.
5. World Meteorological Organization, Global Ozone Research and Monitering Project-Report no. 20: Scientific Assessment of Stratospheric Ozone, Volume I. WMO, NASA, NOAA, UNEP and UKDOE, 1989.
6. Jones, R. L., Austin, J., McKenna, D. S., Anderson, J. G., Fahey, D. W., Farmer, C. B., Heidt, L. E., Kelly, K. K., Murphy, D. M., Proffit, M. H. and Tuck, A. F. *J. Geophys. Res. 94* (1989) 11529.
7. Basco, N. and Hunt, J. E. *Int. J. Chem. Kinet. 11* (1979) 649.
8. Cox, R. A. and Hayman, G. D. *Nature (London) 332* (1988) 796.
9. Hayman, G. D., Davies, J. M. and Cox, R. A. *Geophys. Res. Lett. 13* (1986) 1347.
10. McGrath, M. P., Clemitshaw, K. C., Rowland, F. S. and Hehre, W. J. *J. Phys. Chem. 94* (1990) 6162.
11. Sander, S. P., Friedl, R. R. and Yung, Y. L. *Science 245* (1989) 1095.
12. Molina, M. J., Colussi, A. J., Molina, L. T., Schindler, R. N. and Tso, T.-L. *Chem. Phys. Lett. 173* (1990) 310.
13. Burkholder, J. B., Orlando, J. J. and Howard, C. J. *J. Phys. Chem. 94* (1990) 687.
14. Birk, M., Friedl, R. R., Cohen, E. A., Pickett, H. M. and Sander, S. P. *J. Chem. Phys. 91* (1989) 6588.
15. Trolier, M., Mauldin, R. L. III and Ravishankara, A. R. *J. Phys. Chem. 94* (1990) 4896.
16. DeMore, W. B. and Tschuikow-Roux, E. *J. Phys. Chem. 94* (1990) 5856.
17. Cheng, B.-M. and Lee, Y.-P. *J. Chem. Phys. 90* (1989) 5930.
18. Jensen, F. and Oddershede, J. *J. Phys. Chem. 94* (1990) 2235.
19. Slanina, Z. and Uhlik, F. *Chem. Phys. Lett. 182* (1991) 51.
20. Permien, T., Vogt, R. and Schindler, R. N. In Cox, R. A., Ed. *Mechanisms of Gas Phase and Liquid Phase Chemical Transformations*, Air Pollution Rep. No. 17, Environmental Research Program of the CEC, EUR 12035 EN, Brussels 1988.
21. Nickolaisen, S. L., Friedl, R. R. and Sander, S. P. *J. Phys. Chem. 98* (1994) 155.
22. Hansen, K. B., Wilbandt, R. and Pagsberg, P. *Rev. Sci. Instrum. 50* (1979) 1532.
23. Nielsen, O. J. Risø-R-480, Risø National Laboratory, Roskilde 1984.
24. Ellermann, T. Risø-M-2932, Risø National Laboratory, Roskilde 1991.
25. Rasmussen, O. L. and Bjergbakke, E. Risø-R-395, Risø National Laboratory, Roskilde 1984.
26. Bodenstein, M. and Kisteakowsky, G. B. *Z. Phys. Chem. 116* (1925) 372.
27. Lin, C.-L. *J. Chem. Eng. Data 21* (1976) 411.
28. Knauth, H.-D., Alberti, H. and Clausen, H. *J. Phys. Chem. 83* (1979) 1604.
29. Molina, L. T. and Molina, M. J. *J. Phys. Chem. 82* (1978) 2410.
30. DeMore, W. B., Sander, S. P., Golden, D. M., Molina, M. J., Hampson, R. F., Kurylo, M. J., Howard, C. J. and Ravishankara, A. R. Chemical Kinetics and Photochemical Data for use in Stratospheric Modelling. NASA-Jet Propulsion Laboratory, CA, JPL Publ. 90-1, 1990.
31. Simon, F. G., Schneider, W., Moortgat, G. K. and Burrows, J. P. *J. Photochem. Photobiol. A 55* (1990) 1.
32. Watson, R. T. *J. Phys. Chem. Ref. Data 6* (1977) 871.
33. Stevens, P. S. and Anderson, J. G. *J. Phys. Chem. 96* (1992) 1709.
34. Troe, J. *J. Phys. Chem. 83* (1979) 1.
35. Baulch, D. L., Duxburry, J., Grant, S. J. and Montaque, D. C. *J. Phys. Chem. Ref. Data 10* (1981) suppl. 1,1-1.
36. McPherson, M. T., Pilling, M. J. and Smith, M. J. C. *J. Phys. Chem. 89* (1985) 2268.
37. Wallington, T. J., Dagaut, P. and Kurylo, M. J. *Chem. Rev. 92* (1992) 667.

Received May 24, 1994.